Fabrication and Characterization of Eco-Friendly CaO-Modified Cellulose Acetate Fibers via Electrospinning for Potential Biomedical Applications

Wasan Alkaron[1,2,3*], Tamás Kolonits[1], Katalin Balázsi[1] and Csaba Balázsi[1*]

[1] Institute of Technical Physics and Materials Science, HUN-REN Centre for Energy Research, Konkoly-Thege, Miklós Str. 29-33, 1121 Budapest, Hungary

[2] Doctoral School of Materials Science and Technologies, Óbuda University, Bécsi Str. 96/B, 1030 Budapest, Hungary

[3] Technical Institute of Basra, Southern Technical University, Basra 61001, Iraq

*Correspondence author email: wasan.alkaron@ek.hun-ren.hu and balazsi.csaba@ek.hun-ren.hu

Abstract

New eco-friendly fiber composites were developed by electrospinning cellulose acetate (CA) combined with calcium oxide (CaO) derived from thermally treated waste eggshells. CA solutions were prepared at varying concentrations to optimize the ideal concentration for producing smooth, continuous, and beads-free fibers. Various amounts of CaO were then added to assess its impact on fiber structure, crystallinity, and swelling characteristics.

FTIR examinations demonstrated that CaO was effectively integrated without altering the CA structure, however XRD investigations revealed reduction in crystallinity with increasing CaO content. The swelling capacity remarkedly increased to 710% at 4% CaO, attributed to enhanced porosity and hydrophilicity, before showing a slight decline at higher concentrations due to particle aggregation. These results highlight a sustainable method for producing functional CA/CaO composites with tailored properties for promising applications in biomedical and environmental fields. Our further aim is to study the biocompatibility, cytotoxicity and the photocatalytic activity of the prepared composites.

Keywords: Waste eggshells; electrospinning; fiber composite.

1. Introduction

Nowadays, there is a growing demand for environmentally sustainable alternatives to petroleum-derived polymers, which are designed to enhance biological compatibility while retaining structure flexibility and performance [1], [2], [3], [4]. Bio based polymers, derived from renewable sources such as plants and microbes, emerge as viable alternatives for biomedical applications owing to their basic biodegradability, biocompatibility, and low environmental impact [5], [6]. The structural variety and functional versatility of these materials make them particularly suitable for advanced production methods like electrospinning, which produces fibrous architecture that closely mimic the extracellular matrix (ECM) [7], [8]. Among the various biopolymers, cellulose derivatives, especially cellulose acetate (CA), have attracted considerable interest. CA is known for its excellent mechanical properties, chemical stability, and ease of processing, making it an ideal foundation for creating biomedical materials such as wound dressings, tissue engineering scaffolds, and drug delivery systems [9], [10], [11]. Electrospinning has become a highly efficient method for creating CA fibers characterized by a large surface area and interconnected porosity, which are essential attributes for biomedical scaffolds, wound healing applications, and filtration systems [12], [13], [14].. The incorporation of eco-friendly fillers derived from natural, or waste sources has become an effective strategy to improve polymer functionality and presents an environmentally friendly and economical approach to transform biowaste, while simultaneously adding crucial minerals to composite systems. Eggshells are an abundant by-product of the food industry, generated in millions of tons annually worldwide. Eggshells are consisting mainly of $CaCO_3$ (94–97%), which can be converted into high-purity CaO through simple calcination process without the use of any chemical. This harmful-chemical-free conversion method can be considered a green synthesis route making this a cost-effective and sustainable waste to value process [12], [13]. CaO is notable for its ability to reinforce structures due to its remarkable properties, such as high biocompatibility, superior bioactivity, and chemical reactivity [15]. In comparison to other environmentally friendly fillers like biochar, plant ash, clay minerals, or bone-derived hydroxyapatite, eggshell-derived CaO plays a crucial role in biomedical and functional applications [16]. These particles significantly improve osteoconductivity and promote new bone growth, rendering them exceptional candidates for bone tissue engineering [17], [18], [19]. When exposure to water or physiological fluids, CaO readily hydrates to form calcium hydroxide ($Ca(OH)_2$), releasing hydroxyl ions that increase local alkalinity. Simultaneously, it provides an elevated, antibacterial pH environment, neutralizes acidic degradation products in polymers, and

releases calcium ions that are beneficial for bone and teeth regeneration, dental therapies, and wound healing [20]. Moreover, CaO shows strong affinity for phosphate and carbonate ions when immersed in physiological media, facilitating the formation of calcium phosphate phases such as hydroxyapatite ($Ca_{10}(PO_4)_6(OH)_2$) which is a crucial component of bone and teeth, providing them with strength and rigidity [21].

Using eggshell-derived CaO also has clear environmental advantages over CaO sourced from conventional sources. Commercial CaO is usually obtained through mining and calcining limestone, processes associated with land disturbance, high energy demands, and significant CO_2 emissions [22]. Recent research trends focused on developing innovative processes to prepare a variety of biomaterials using biowastes instead of costly synthetic reagents and hazardous chemicals [16] [23]. Although several studies have explored CaO or eggshell-derived fillers, most of this research has been directed towards their use on applications such as adsorbents, catalysts, or high-temperature CO_2 capture [24], [25]. To our knowledge, there is no research on the incorporation of waste-derived CaO into CA fiber composites, particularly about evaluating how CaO influences fiber morphology, swelling, and surface characteristics relevant for potential functional applications. Therefore, the novelty of this work lies in: (i) integrating eggshell-derived CaO as a sustainable and cost-effective filler source into CA fibers using the electrospinning technique, and (ii) demonstrating how CaO content and processing conditions affect the structural and physicochemical properties of the resulting composite.

A primary limitation in the production of these composites is achieving a uniform dispersion of particles. The robust van der Waals forces sometimes lead to the aggregation of particles, thereby affecting the uniformity of the fibers and their functional characteristics. Consequently, controlled adjustment of solution composition, electrospinning parameters and dispersion methods is important to facilitate the optimal incorporation of CaO into electrospun CA fibers while maintaining their favorable morphological properties [26], [27].

The present study focuses on creation eco-friendly CA/CaO fibers composite using CaO particles obtained from calcined waste eggshells. The electrospinning concentration was optimized utilizing a 15 wt% CA solution in a 2:1 acetone-to-acetic acid solvent system, which produced homogeneous, bead-free fibers with favorable morphological and structural characteristics. The addition of CaO modified the crystallinity and decreased the fiber diameter, and clearly affected hydrophilicity and swelling behavior, with maximal improvement noted at 4% CaO loading.

2. Materials and methods

2.1 Materials

Cellulose acetate (CA) with an average molecular weight of 29,000 g/mol, an acetyl content of 40 wt%, and a substitution degree of approximately 2.4 was obtained from Sigma-Aldrich (USA). Acetone (Fisher Chemicals, Finland) and acetic acid (VWR Chemicals, Finland) used as a solvent to prepare the spinning solution. All chemicals and solvents were used as supplied, without any further purification or alteration. Calcium oxide (CaO) was prepared from calcining chicken eggshells.

2.1.1. Preparation of CaO from eggshell

Initially, the eggshells were thoroughly washed with distilled water to eliminate any organic residues and then left to air-dry at room temperature. Then, the eggshells were crushed and ground into a consistent powder using a mortar and ball mill followed by sieving through a 40 μm mesh to achieve uniform particle size and sample consistency. The powders were then exposed to thermal treatment in a furnace at 900 °C for 12 hours, these calcination conditions were chosen based on previous experimental experience and literature reporting that this temperature range ensures complete decomposition of $CaCO_3$ into CaO [28]. The resultant powder cooled to ambient temperature and stored in a sealed container to minimize moisture effect.

2.1.2. Preparation of Cellulose Acetate (CA) Fibers by Electrospinning

CA fibers were created through the electrospinning process. To achieve a uniform polymer solution, CA powder was initially dissolved in a solvent blend of acetone and acetic acid, maintaining a 2:1 volume ratio. The solvent system of 2:1 acetone/acetic acid was selected based on our previous studies [29], which provides polymer solubility, and suitable viscosity for electrospinning. CA solutions were prepared at four concentrations (w/v), 5%, 10%, 15%, and 20% (w/v) to determine the optimal concentration for producing long, smooth, and continuous fibers.

Following that, the solutions were loaded into 10 ml syringes with stainless steel needles having an internal diameter of 0.95 mm. These syringes were connected to a syringe pump, which controlled the flow rate of the solution as it was dispensed. The electrospinning process was carried

out using a standard vertical setup (Electrospinning equipment model NE100 from Inovenso Electrospinning Co., Turkey). An aluminum foil-covered static collector was positioned 10 cm from the needle's tip with a constant voltage of 20 kV, and a flow rate of 1.0 mL/h was maintained during this process. All electrospinning experiments were carried out at ambient temperature and atmospheric pressure. Among the tested concentrations, the one yielding the most uniform and bead-free fibers was considered optimal for further use.

2.1.3. Preparation of CA/CaO composite fibers

Preliminary optimization demonstrated that a 15% (w/v) CA solution in a 2:1 (v/v) acetone–acetic acid solvent system produced uniform, bead-free fibers. To fabricate bioactive composite fibers, CaO particles obtained from the calcinated eggshells at 900 °C for 12 hours were incorporated into the CA solution at varying concentrations of 2%, 4%, and 6% (wt) relative to the polymer weight. The CaO powder was first dispersed in the solvent mixture and then added to the CA solution under continuous stirring to form a homogeneous suspension. Each composite solution was electrospun under optimized conditions of an applied voltage of 20 kV, flow rate of 1.5 mL/h, and a tip-to-collector distance of 10 cm, to produce CA/CaO composite fiber mats and resultant fibers were gathered and examined. The schematic representation of preparation methods is summarized in Figure (1).

(a)

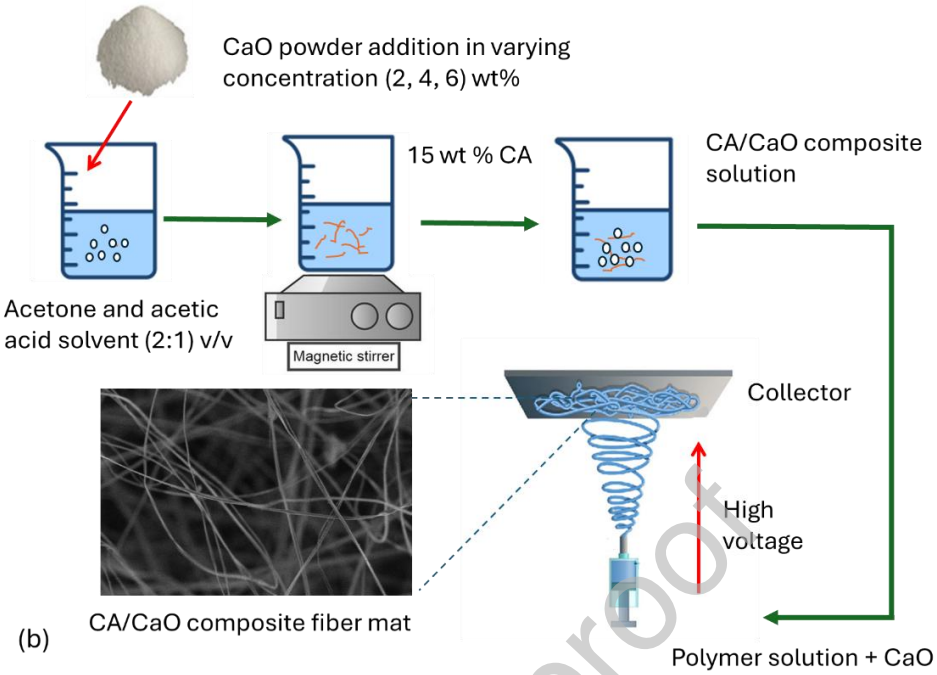

Figure (1) Schematic diagram of the preparation methods: (a) step process step of CaO synthesizing particles from eggshell, and (b) electrospinning process of CaO/CA biopolymer composites.

3. Characterization methods

The morphological characteristics of raw and calcined eggshell powders were examined utilizing field-emission scanning electron microscopy (FE-SEM; Thermo Scientific Scios2, Waltham, MA, USA). The elemental content and distribution were evaluated using energy-dispersive X-ray spectroscopy (EDS; Oxford Instruments X-MaxN detector, Abingdon, UK). Furthermore, the structure of both pure and CA/CaO composite fibers at different concentrations were evaluated via SEM imaging and EDS to investigate the distribution of CaO within the fiber matrix.

To explore possible chemical interactions between CA and CaO, fourier-transform infrared spectroscopy (FTIR) was utilized. The infrared spectroscopic analysis was carried out using the attenuated total reflection (ATR) method. A Varian Scimitar 2000 FT-IR spectrometer (Varian Inc., Palo Alto, CA, USA) equipped with an MCT (mercury–cadmium–telluride) detector was used and fitted with a 'Golden Gate' single reflection diamond ATR unit (Specac Ltd., Cray Ave, Orpington, UK). During the measurements, the solid samples, without any sample preparation, were pressed with a constant 70 cN/m^2 pressure on the top of the diamond ATR crystal by a sapphire anvil. All spectra were collected with a nominal resolution of 4 cm^{-1} by the co-addition of 128 individual spectra. Before spectral evaluation, ATR correction was performed.

X-ray diffraction (XRD; Bruker AXS D8 Discover, Karlsruhe, Germany) equipped with a Cu Kα radiation source (λ = 0.154 nm), Göbel mirror, and scintillation detector (operated at 40 kV and 40 mA), was used to identify crystalline phases in the calcined eggshells and CA/CaO composite fibers. Phase identification and crystallographic analysis were performed using Diffract Eva software.

Swelling behavior was assessed to determine water uptake capacity. Square samples (2 × 2 cm²) of CA and CA/CaO mats were immersed in distilled water for 24 h, gently blotted to remove surface moisture, weighed (W), then vacuum-dried at 50 °C for 1 h and reweighed (W_d). The swelling percentage was calculated using the following equation:

$$\text{Swelling (\%)} = \frac{W - W_d}{W_d} x100 \qquad (1)$$

Where, W is the mass after immersion, and W_d is the dry mass post-drying.

4. Results and Discussion

4.1. Morphological and structural characterization of raw and calcined eggshells

Figure (2) shows the morphological, elemental, and structural characterization of both untreated eggshell powder and its calcined form. The findings provide a comprehensive understanding of the conversion process from biogenic $CaCO_3$ to CaO through heat treatment.

The SEM image of raw eggshell powder shows an irregular, plate-like microstructure with relatively smooth surfaces and sharp, fractured edges. Particle sizes exhibit considerable variability, indicative of the heterogeneous and fragile characteristics of crushed eggshells, primarily constituted of crystalline $CaCO_3$ in the calcite form. The microstructure exhibits compactness and rigidity characteristic of unrefined bioceramic material with low porosity [30], [31].

By calcination at elevated temperature (900 °C for 12 hours), morphology undergoes substantial alteration. The surface exhibits higher porosity due to fine-grained particles forming a brittle and fragile structure. This alteration is caused by the heat decomposition of $CaCO_3$ into CaO, which releases CO_2 gas, resulting in volume reduction and microstructural change [32], [33]. EDS mapping verifies the elemental composition of the calcined product as shown in Figure (2,

c)Calcium (Ca), depicted in green, is the predominant element and is evenly distributed across the sample, confirming complete thermal transformation. Oxygen (O) is abundant, aligning with the creation of CaO. Carbon (C) is present in a minimal amount, possibly due to environmental exposure. Trace amounts of magnesium (Mg) and sulfur (S) are also present, which are typically found in eggshells and have previously been found in eggshell-derived biofillers as shown in Table (1). [33], [34]. The standard XRD pattern of untreated eggshell exhibits prominent peaks that signify crystalline $CaCO_3$, specifically in the calcite phase. The peaks clearly indicate that biogenic calcium carbonate is structured in a crystalline and ordered manner [35]. XRD patterns after calcination Figure (2, d) revealed a pronounced diffraction peak associated with CaO rather than $CaCO_3$ peaks, indicating a successful thermal breakdown reaction [36], [37].

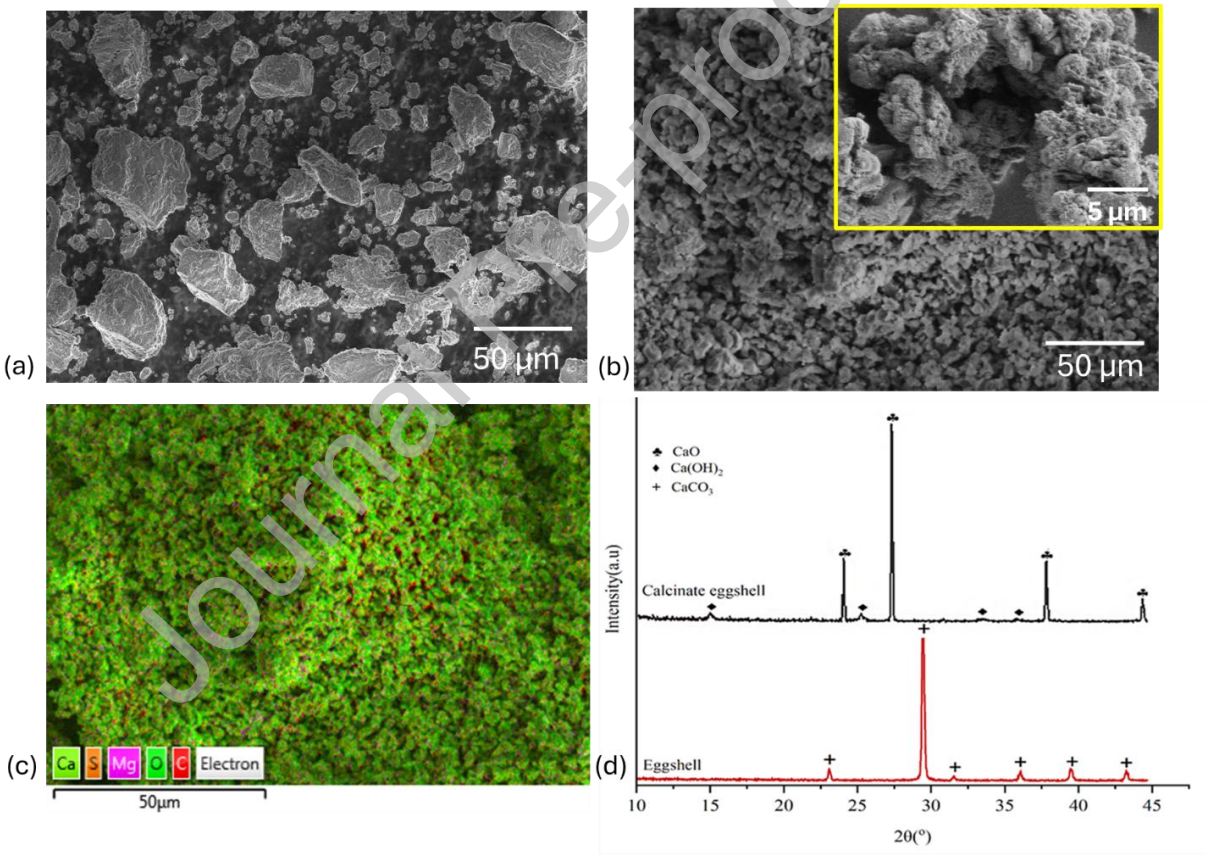

Figure (2) SEM images of (a) raw eggshell powder, and (b) calcined eggshell powder; (c) the corresponding EDS elemental mapping image of the calcined eggshell powder, and (d) XRD patterns comparing raw and calcined eggshell.

Table (1) Elemental composition of raw and calcined eggshell

Element	Raw eggshell weight%	Calcined eggshell weight%
C	31.39	12.24
O	48.09	56.09
Ca	18.45	30.88
Mg	0.23	0.58
N	1.31	-----
P	0.09	trace
S	0.37	0.08
Na	0.09	trace

In addition, there are minor peaks of $Ca(OH)_2$, likely caused by hydration of CaO during storage or handling [38]. There are several research works in which the authors have proven that controlled calcination of biogenic $CaCO_3$ results in the conversion of CaO with high purity and reactivity according to prior literature [39], [40], [41], [42], [43].

4.2. Morphological investigation of electrospun CA fibers

SEM was employed to evaluate the CA fibers from solutions of varying concentrations 5%, 10%, 15%, and 20% (w/v) using a 2:1 (v/v) mixture of acetone and acetic acid. On Figure (3) it clearly shows how the concentration of the polymer affects fiber morphology, revealed a clear transition from bead-rich structures to smooth, continuous fibers as the concentration increases.

At lower concentration of 5 wt%, the electrospining solution exhibits inadequate viscosity and chain entanglement, leading to bead-dominated structures instead of continuous fibers. The morphology consists of several spherical beads and droplets, signifying an unstable jet during electrospinning. This behaviour is characteristic of dilute polymer solutions, where surface tension prevails over viscoelastic forces, resulting in electrospraying rather than appropriate fiber production. This behavior aligns with well-established electrospinning regime of Sayed et.al and Deitzel et.al [44], [45] producing droplets or beads due to low viscosity and chain entanglement.

It was found that increasing CA concentration to 10% partial fiber formation occurs. It can be observed from the SEM image of Figure (3) that thin, irregular fibers begin to form with average fiber diameter of 0.268 µm as shown in Figure (4), interspersed with beads of varying sizes. While

the solution exhibits improved spinnability compared to 5%, the fiber network is still inconsistent, and many defects are present. The concentration is therefore near the threshold for stable fiber formation but remains below the optimal viscosity for fiber formation. Well-documented findings exist on this transition behavior. Tarus et al. [46] observed that at approximately 10 wt% CA in an acetone/DMAc solution, fibers with beads linked by delicate threads are formed. Similarly,, research on polymer systems indicates that when the concentration exceeds the entanglement threshold but does not reach an optimal level, bead-on-string structures appear due to inadequate chain overlap and viscosity [47], [48].

With CA concentration raised to 15 wt%, the electrospun fibers show a uniform, bead-free morphology with consistent fiber diameters of 2.209 μm as presented in Figure (3) and Figure (4). The fibers are smooth, well-aligned, creating a homogeneous mat. This finding is consistent with previous studies. A systematic study of CA electrospinning with trifluoroacetic acid demonstrated that concentrations between 13–15 wt% produced smooth, bead-free fibers under ideal electrospinning conditions [49]. A comparative examination covering 5–20% (w/v) CA demonstrated that continuous fibers began to form at around 10%, but it was only at approximately 17% that a consistently bead-free and uniform morphology was achieved [50].

At 20 wt%, the fiber morphology begins to deteriorate again. Fibers appear thicker (average fiber diameter 3.384 μm) and flatter, with ribbon-like structures and irregular surfaces. In this instance, high viscosity inhibits jet stretching and solvent evaporation, resulting in fiber flattening or merging upon deposition. Such behavior is extensively documented in electrospinning research. Celebioglu and Uyar [51] noted that ribbon-like fibers can develop when using highly volatile solvents or when the polymer solution has high viscosity, both of which encourage the rapid formation of a surface skin that collapses into ribbons. A higher polymer concentration further intensifies this effect, limiting the jet's capacity to fully elongate. Dhanalakshmi et al. [52] observed flat ribbon shapes in Nylon 11 when the concentration rose to approximately 20 wt%, attributing this change to high viscosity, which restricts jet instability and effective solvent evaporation.

Fiber diameter analysis Figure (4) revealed that fiber diameters increased systematically with solution concentration. Specifically, the average diameter increased from 0.268 μm (10 wt%) to 3.384 μm (20 wt%) because higher concentration increases the solution viscosity and the degree

of polymer chain entanglement. When viscosity is higher, the electrospinning jet experiences greater hindering fiber stretching and resulting in thicker fibers [53].

In conclusion, optimizing polymer concentration is crucial for achieving desired electrospun fiber characteristics. At lower concentrations of 5 wt%, insufficient chain entanglement allows jet breakup and bead formation, whereas at higher concentrations 20 wt% the excessive viscosity of the solution led to rapid needle tip clogging and premature polymer solidification at the spinneret. In contrast, 15 wt% is the optimal concentration under electrospinning conditions, offering the right combination of viscosity, chain entanglement, and jet stability to produce defect-free fibers.

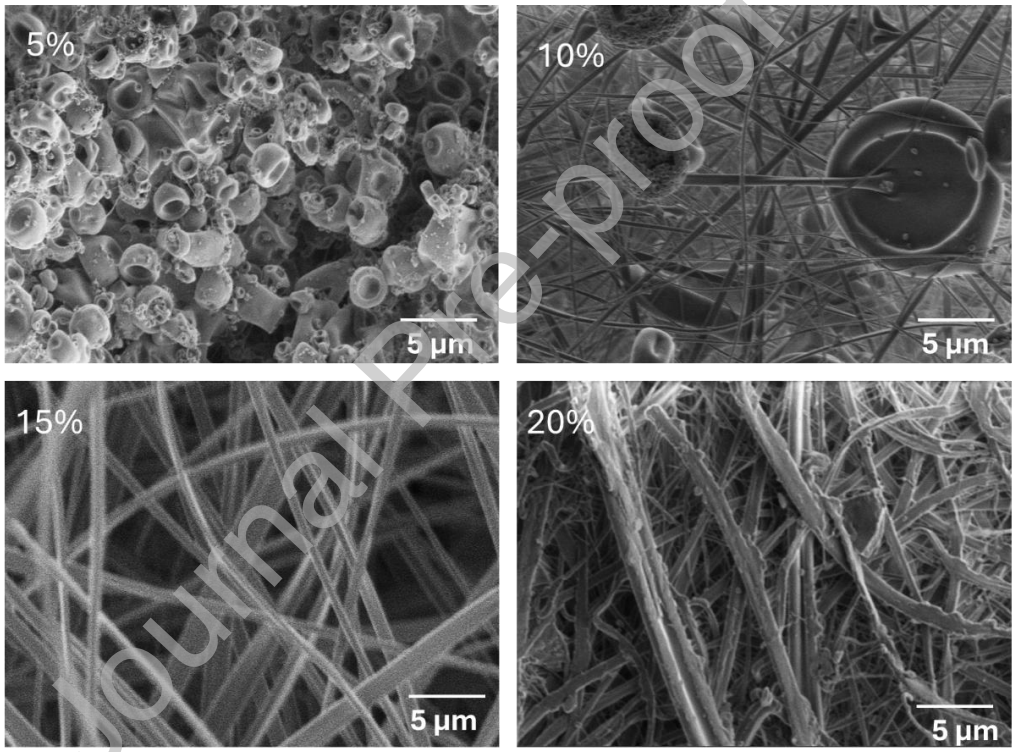

Figure (3) SEM images of electrospun CA fibers in (2:1) acetone/acetic acid at different concentrations: 5, 10, 15, and 20 %.

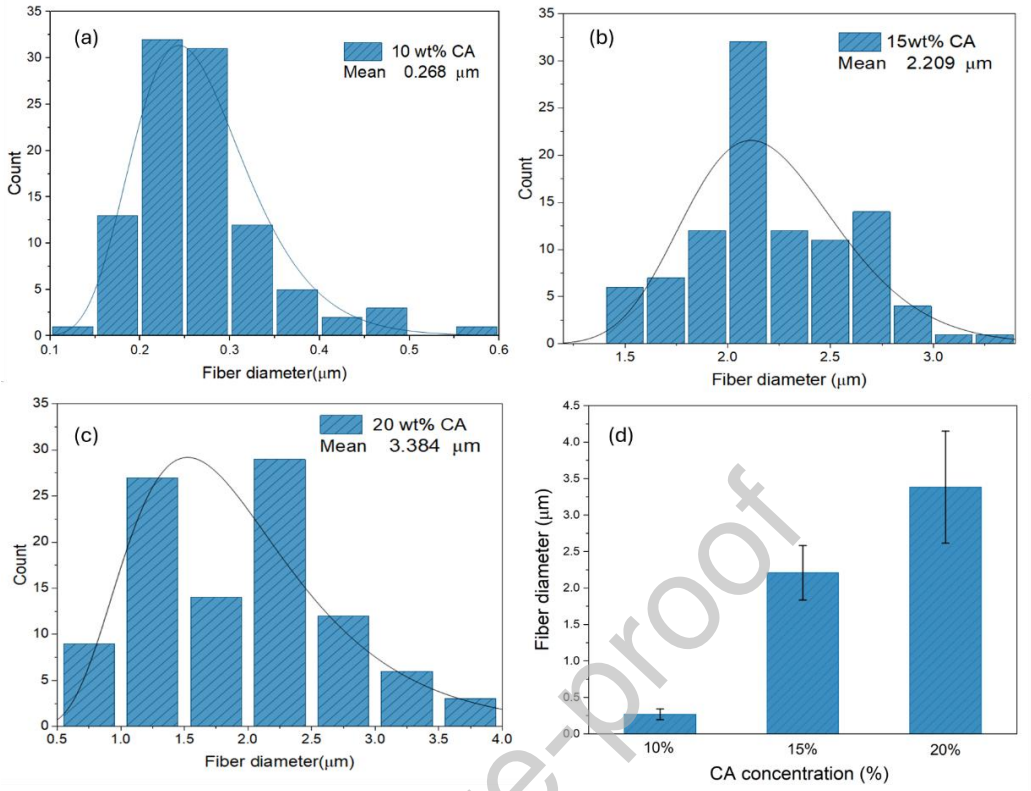

Figure (4) Corresponding fiber diameter distribution of CA at various concentrations (a) 10%, (b) 15%, (c) 20%, and (d) Variation of fiber diameter vs. CA concentration,

4.3. Morphological and structural investigation of CA/CaO electrospun fibers

According to morphological investigation of electrospun CA fiber, 15% concentration of CA exhibited a uniform and bead-free structure, which was therefore selected for producing composite fibers incorporating CaO derived from calcined eggshell. Figure (5) illustrates the morphological and elemental characterization of the composite fibers produced with different CaO loadings of (0, 2, 4, and 6) wt% relative to polymer content.

Electrospun pure CA fibers exhibited a smooth, bead-free morphology with uniform and continuous fibers, having an average diameter of 2.209 µm. The EDS spectrum identified only carbon (C) and oxygen (O), aligning with the anticipated composition of pure CA, and verified the absence of calcium (Ca) or any inorganic contaminants. Vanjari et al. [54] reported similar results, showing through EDS spectroscopy that pure membranes CA contain only C and O, without any detectable inorganic fillers or impurities.

The addition of 2% CaO maintained structural integrity and resulted in a considerable reduction of the mean fiber diameter to 0.895 μm. The EDS spectra confirmed the successful presence of Ca, in addition to C and O, showing the uniform integration of CaO particles into the polymer matrix. The reduction in fiber diameter may correspond to the improved electrical conductivity of the polymer solution caused by the CaO particles, which promotes increased elongation of the electrospinning jet under the applied electric field, an effect thoroughly documented in particles-modified electrospinning systems [55]. Comparably, Schofield et al. [56] revealed that the integration of $AgTiO_2$ particles into poly(3-hydroxybutyrate) (PHB)/gelatin composites significantly reduced fiber diameter owing to enhanced solution conductivity. Similarly, Malakhov et al. [57] indicated that incorporating metal stearate, such as calcium stearate, into polypropylene (PP) during electrospinning, significantly enhanced electrical conductivity, and yielding finer fiber diameters.

4% CaO loading resulted even fine fibers with an average diameter of 0.528 μm with a bead-free morphology. EDS results showed an enhanced Ca signal, confirming the increased CaO incorporation, and SEM images showed no signs of aggregation or defects in the beads. The enhancement in fiber fineness and consistency implies that a moderate amount of particles improves jet stability and stretching, without exceeding the limit that would negatively affect spinning performance.

Upon reaching a CaO concentration of 6%, the average fiber diameter further reduced to 0.294 μm, the smallest recorded among all evaluated formulations. At this elevated filler loading, SEM images revealed slight fiber fusion and surface roughness in some regions. This behavior may be due to heightened viscosity and the possibility of particles agglomeration [55]. In spite of this, EDS confirmed a strong calcium signal, indicating the successful incorporation of the highest CaO concentration.

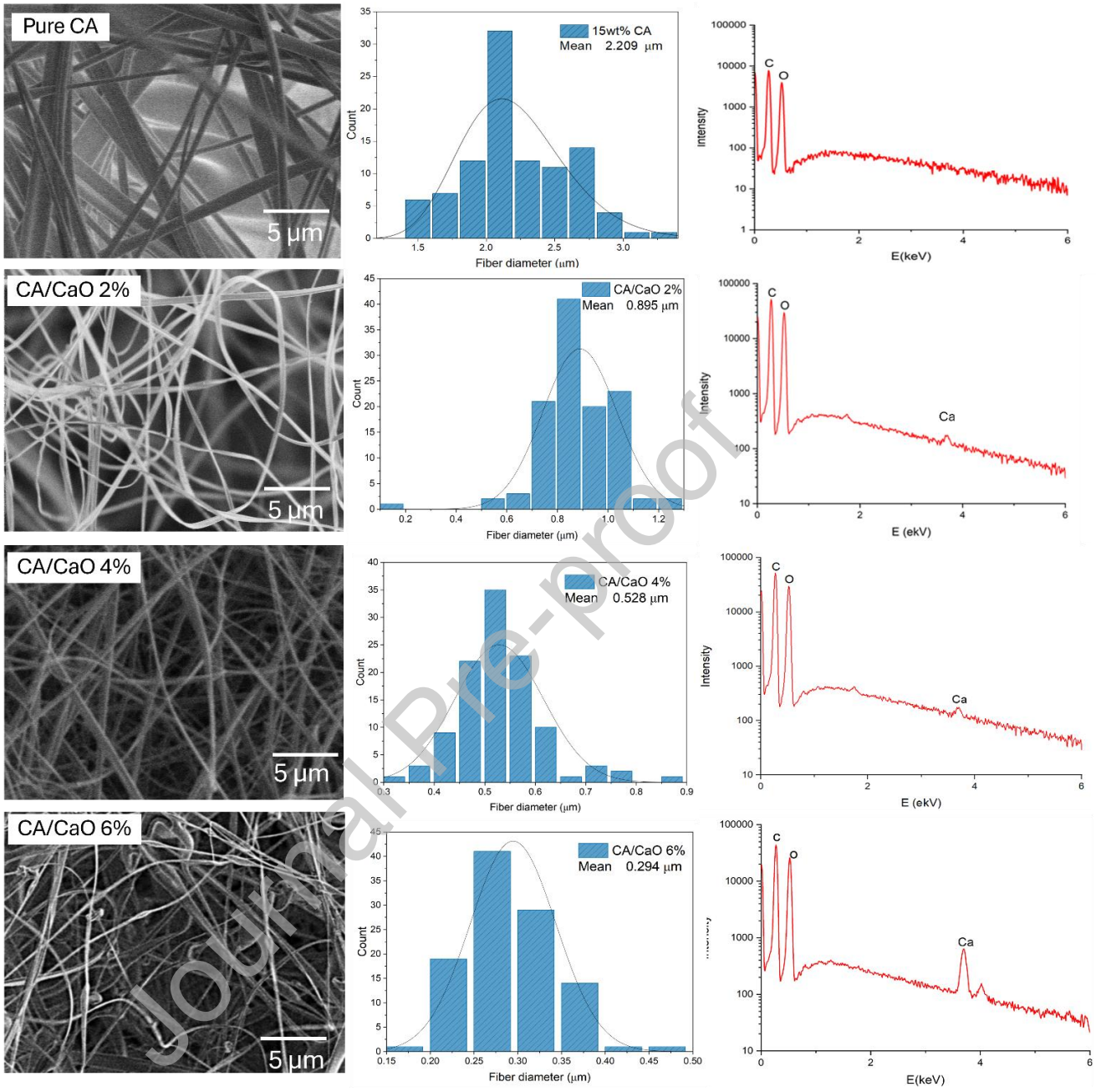

Figure (5) SEM images, fiber diameter distributions, and EDS spectra of electrospun CA/CaO composite fibers at different CaO concentrations.

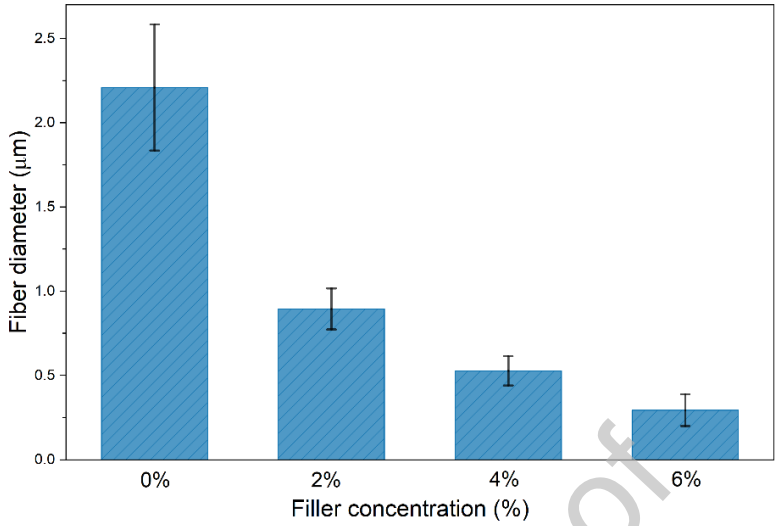

Figure (6) Effect of CaO filler concentration on average fiber diameter.

The results show an inverse relationship between CaO content and fiber diameter, with greater CaO loading leading to finer fiber production Figure (6). The reduction in fiber diameter with increasing CaO content can be attributed to changes in the spinning solution properties. The presence of CaO particles likely increases the electrical conductivity of the solution, which enhances electrostatic stretching of the jet and results in finer fibers. Similar findings reported in previous studies demonstrate that particles can affect solutions' viscosity and conductivity, which in turn decrease fiber formation during electrospinning [58]. In addition, the gradual increase of calcium peak intensity in the EDS spectra of the composite samples verifies the effective and well distribution of CaO particles within the CA fibers.

4.4. FTIR analysis

The FTIR spectral properties of pure CA, CaO, and CA/CaO composite fibers containing 2%, 4%, and 6% CaO offer important insights into the molecular structure, functional groups, and potential interactions between CA and CaO within the composite fiber systems (Figure 7).

The spectrum of pure CA reveals specific bands that signify its acetylated cellulose structure. A broad band centered around 3480 cm^{-1} is associated with O–H stretching vibrations, which relate to the remaining hydroxyl groups. The significant band near 2950–2850 cm^{-1} is due to the C–H stretching of aliphatic $–CH_3$ and $–CH_2–$ groups. The prominent peaks shown at between 1750–1730 cm^{-1} is a result of the C=O stretching vibration of the ester (acetyl) functionalities. The

additional peaks observed at 1370 cm^{-1} and 1220 cm^{-1} are attributed to C–H bending and C–O stretching, respectively. Additionally, the range of 1030–1040 cm^{-1} is linked to C–O–C asymmetric stretching within the polysaccharide structure. These spectral profiles verify the chemical integrity and successful electrospinning of CA fibers. The observed assignments are in agreement with previously reported FTIR studies that report similar band positions and confirm the chemical integrity of acetylated cellulose in electrospun fiber [55], [59].

The FTIR results revealed that the spectrum of CaO displays two broad absorption bands in the range of 1000–1500 cm^{-1}, which is attributed to Ca–O lattice vibrations. This suggests the successful transformation from $CaCO_3$ to CaO [60], [61]. In addition, CaO exhibits a small and sharp absorption peak at around ~3700 cm^{-1} which is attributed to the surface-adsorbed O–H groups, from minor hydration or atmospheric moisture [62].

When CaO is added to the CA matrix, the composite spectra (2%, 4%, and 6% CaO) maintains the primary functional groups of CA without notable shifts in the main CA peaks, suggesting that the essential chemical structure of CA remains intact. However, new absorption bands are observed, especially in the 500–1000 cm^{-1} range and around 1250–1750 cm^{-1} (as indicated by black arrow). These features are characteristic of Ca–O vibrational modes and suggest that CaO particles are effectively integrated and well-dispersed into the polymer matrix [55].

The relative intensity of peaks associated with Ca–O increases steadily as the CaO content rises, with the 4% and 6% composites exhibiting the most distinct CaO-related characteristics. This indicates enhanced dispersion and stronger interfacial interactions at these concentrations. Crucially, there are no notable shifts in the CA backbone signals, confirming that the addition of CaO does not alter the fundamental polymer structure. Instead, it may improve interfacial bonding through physical interactions like hydrogen bonding or electrostatic interactions.

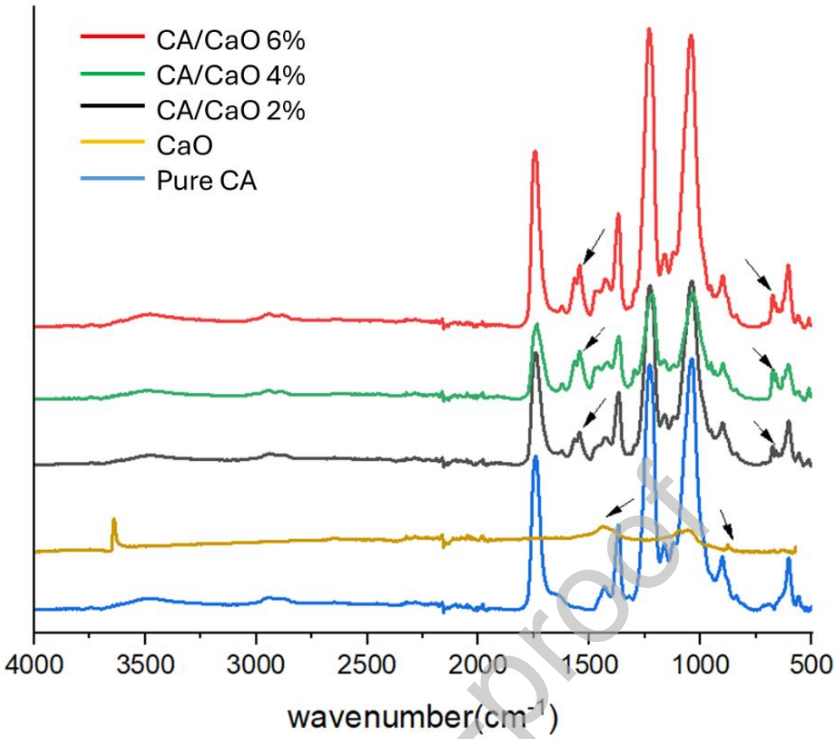

Figure (7) FTIR spectra of CA and CA/CaO electrospun fibers at different CaO concentrations.

4.5. XRD analysis

XRD measurement was conducted to assess the crystalline and phase composition of the electrospun fibrous matrices made from CA and CA/CaO composites, as depicted in Figure (8). The diffraction pattern of pure CA reveals a broad feature centered at roughly $2\theta \approx 21.5°$, indicating its semicrystalline nature and dominated by amorphous regions. This is due to the quick evaporation of the solvent during the fiber formation process. This broad characteristic corresponds with previous findings on electrospun CA, displaying a broad halo around $2\theta \approx 21–22°$ were attributed to limited crystalline ordering within the amorphous polymer [63] [64]. Significant alterations in the XRD patterns are evident upon the addition of CaO. When the CaO concentration is 2%, a slight reduction in intensity is observed, and as the CaO load increases to 4% and 6% the intensity of the broad CA peak lowered and became more diffuse. The effect appears greatest in the CA/CaO 6% sample, characterized by the broadest and least intense diffraction halo. The absence of distinct CaO diffraction peaks suggests well interaction between CaO and CA matrix rather than the formation of large crystalline CaO aggregates [65].

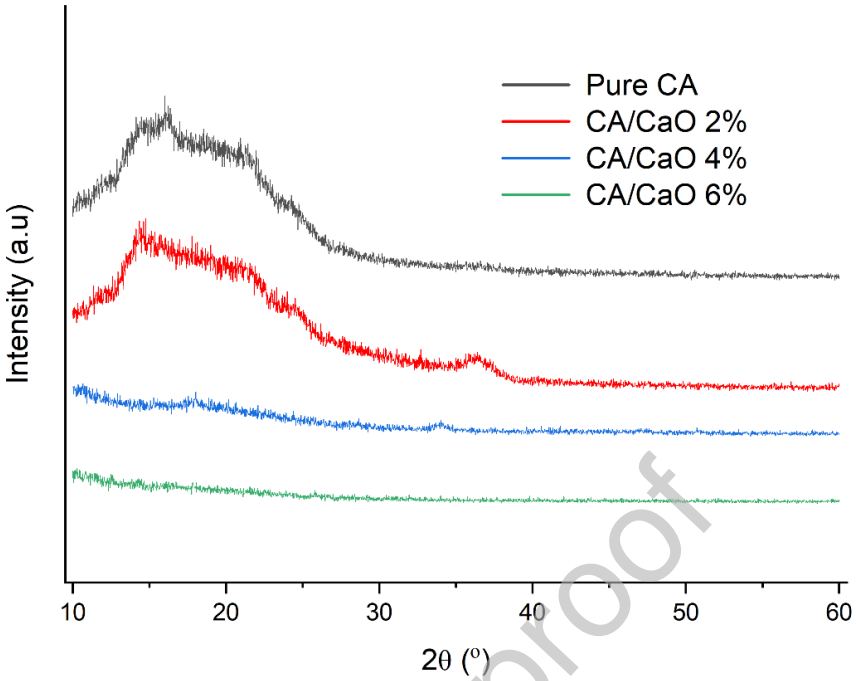

Figure (8) XRD analysis of pure CA and CA/CaO electrospun fibers with varying CaO loading.

4.6. Swelling behavior

Swelling ratio of pure CA fiber mats and CA/CaO composite fiber mats with different CaO loadings (2%, 4%, and 6%) was determined to evaluate how filler incorporating affects hydrophilicity and moisture absorption as illustrated in Figure (9). The swelling rate of pure CA was determined to be approximately 676%, reflecting its inherent hydrophilicity due to polar functional groups [66]. Incorporation of 2% CaO exhibited a modest rise to 685% of swelling rate, indicating a slight increase in water uptake. This improvement results from the well-dispersed CaO particles, which create hydrophilic sites and enhance porosity [67].

At a concentration of 4% CaO, the swelling peaked at 710%, suggesting this is the ideal level where particles greatly improve fiber porosity and promote water diffusion while maintaining structural stability. On the other hand, when the CaO content increased to 6%, the swelling rate slightly reduced to 693%. This reduction may result from particles agglomeration, which can block pore access, reduce effective surface area, and disrupt fiber morphology as evidenced by SEM analysis, which revealed surface roughness and partial fiber fusion. Based on the finding, CA/CaO 4% fibrous mats show the most significant expansion. This study highlights the necessity of

optimizing filler percentages in electrospun composites. Proper filler dispersion enhances hydrophilicity and swelling, whereas excessive loading can disrupt matrix uniformity and restrict solvent access [68].

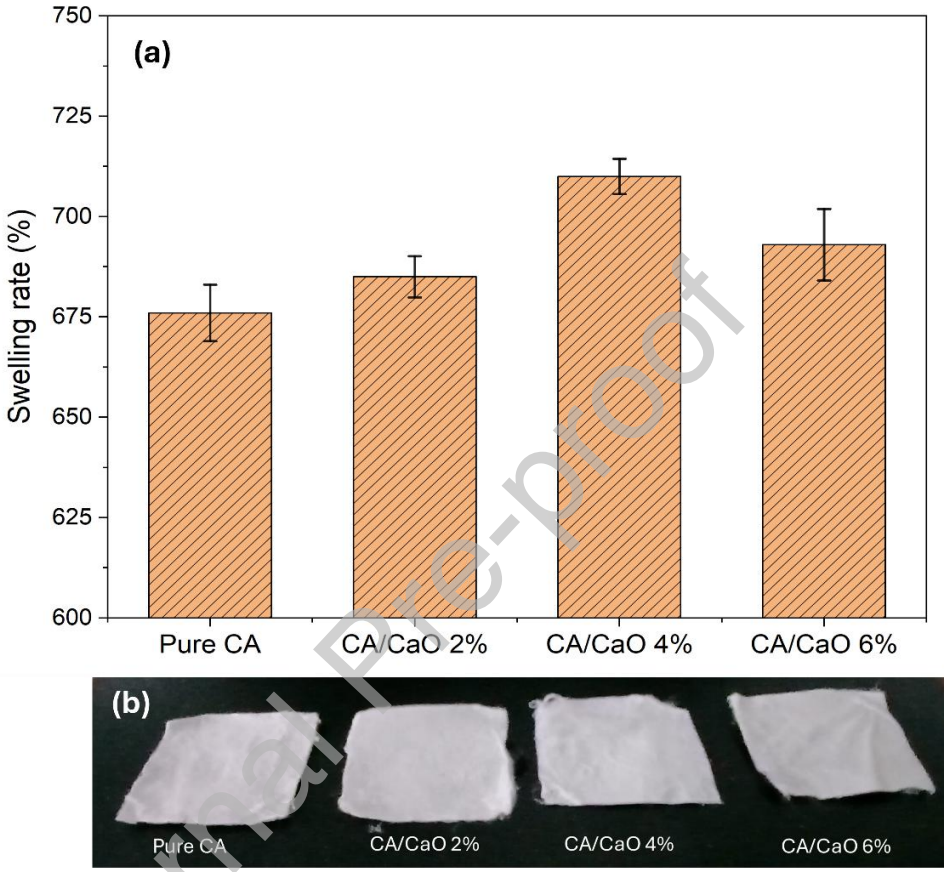

Figure (9) (a) Swelling behavior of pure CA and CA/CaO composites with varying CaO content, and (b) Images of the electrospun fibers mat.

5. Conclusions

In this study, new ecologically friendly CA/CaO composite fibers were successfully developed by electrospinning and employing various CaO concentrations produced by calcining eggshells at 900 °C. SEM, EDS, and XRD investigation confirmed the transformation of $CaCO_3$ into CaO, along with significant morphological and phase changes.

Electrospinning parameters were optimized by varying CA concentration. Using 5–10 wt% CA resulted in fibers with beads, and 20 wt% led to irregular formations. However, 15 wt% CA

produced consistent, bead-free fibers, establishing it as the best formulation in a 2:1 acetone–acetic acid solvent system.

Integrating CaO particles led to a notable decrease in fiber diameter and added bioactive inorganic calcium, all while maintaining the integrity of the fibers. Among the composites, fibers loaded with 4% and 6% CaO showed the most refined morphologies. The 4% CaO-loaded fibers showed the best balance between uniformity and performance, while 6% CaO produced the thinnest fibers.

Analysis via FTIR indicated that CaO was effectively integrated into the CA matrix without altering its intrinsic chemical structure, suggesting interfacial interactions, especially at higher CaO loadings, that could enhance mechanical stability and bioactivity. XRD analysis further demonstrated reduced CA crystallinity upon CaO addition and the presence of CaO-specific features, indicating good particles dispersion.

According to swelling studies, water uptake was increased to 710 at 4% CaO an enhancement of approximately 5%, whereas it decreased slightly to 693 at 6% due to particles agglomeration.
Overall, these findings illustrate the potential of optimized CA/CaO composites, indicated that the electrospun composites exhibit a strong correlation between filler content and structural integrity, along with enhanced swelling behavior and hydrophilicity, positioning them as promising candidates for regenerative therapies and implantable biomaterials. The mechanical and thermal properties of CaO/CA composites will be studied in the future and linked to their surface microstructural, and chemical properties.

Acknowledgement

The project presented in this article is supported by the National Research, Development, and Innovation Office—OTKA NKFI 146076. The authors sincerely thank colleagues from HUN-REN Centre for Energy Research, Viktor Varga and Balázs Erki for their assistance with sample preparation, Dr. Z. E. Horváth for technical assistance with the XRD analysis, and Dr. Kornél Fél for technical assistance with the FTIR analysis of the samples

References:

[1] J. J. Andrew and H. N. Dhakal, “Sustainable biobased composites for advanced applications: recent trends and future opportunities – A critical review,” *Composites Part C: Open Access*, vol. 7, p. 100220, Mar. 2022, doi: 10.1016/j.jcomc.2021.100220.

[2] M. U. Aslam Khan *et al.*, “Recent Advances in Biopolymeric Composite Materials for Tissue Engineering and Regenerative Medicines: A Review,” *Molecules*, vol. 26, no. 3, p. 619, Jan. 2021, doi: 10.3390/molecules26030619.

[3] O. Amponsah, P. S. A. Nopuo, F. A. Manga, N. B. Catli, and K. Labus, “Future-Oriented Biomaterials Based on Natural Polymer Resources: Characteristics, Application Innovations, and Development Trends,” *Int J Mol Sci*, vol. 26, no. 12, p. 5518, Jun. 2025, doi: 10.3390/ijms26125518.

[4] H. S. Samuel, F.-D. M. Ekpan, and M. O. Ori, “Biodegradable, Recyclable, and Renewable Polymers as Alternatives to Traditional Petroleum-based Plastics,” *Asian Journal of Environmental Research*, vol. 1, no. 3, pp. 152–165, Oct. 2024, doi: 10.69930/ajer.v1i3.86.

[5] Y. Xie, S. Gao, D. Zhang, C. Wang, and F. Chu, “Bio-based polymeric materials synthesized from renewable resources: A mini-review,” *Resources Chemicals and Materials*, vol. 2, no. 3, pp. 223–230, Sep. 2023, doi: 10.1016/j.recm.2023.05.001.

[6] R. Kaur, L. Pathak, and P. Vyas, “Biobased polymers of plant and microbial origin and their applications - a review,” *Biotechnology for Sustainable Materials*, vol. 1, no. 1, p. 13, Oct. 2024, doi: 10.1186/s44316-024-00014-x.

[7] A. Kakoria and S. Sinha-Ray, “A Review on Biopolymer-Based Fibers via Electrospinning and Solution Blowing and Their Applications,” *Fibers*, vol. 6, no. 3, p. 45, Jul. 2018, doi: 10.3390/fib6030045.

[8] W. Alkaron, A. Almansoori, K. Balázsi, and C. Balázsi, “Hydroxyapatite-Based Natural Biopolymer Composite for Tissue Regeneration,” *Materials*, vol. 17, no. 16, p. 4117, Aug. 2024, doi: 10.3390/ma17164117.

[9] W. Cheng *et al.*, “Sustainable cellulose and its derivatives for promising biomedical applications,” *Prog Mater Sci*, vol. 138, p. 101152, Sep. 2023, doi: 10.1016/j.pmatsci.2023.101152.

[10] R. V. More, V. Antanitta. S, R. Khonde, and B. Kandasubramanian, “Cellulose and derivatives serving as natural, versatile and biocompatible polymers in biomedical applications,” *International Journal of Polymeric Materials and Polymeric Biomaterials*, vol. 74, no. 10, pp. 923–937, Jul. 2025, doi: 10.1080/00914037.2024.2376247.

[11] S. Iravani and R. S. Varma, “Cellulose-Based Composites as Scaffolds for Tissue Engineering: Recent Advances,” *Molecules*, vol. 27, no. 24, p. 8830, Dec. 2022, doi: 10.3390/molecules27248830.

[12] M. Ahmadi Bonakdar and D. Rodrigue, “Electrospinning: Processes, Structures, and Materials,” *Macromol*, vol. 4, no. 1, pp. 58–103, Feb. 2024, doi: 10.3390/macromol4010004.

[13] W. Alkaron, A. Almansoori, C. Balázsi, and K. Balázsi, “A Critical Review of Natural and Synthetic Polymer-Based Biological Apatite Composites for Bone Tissue Engineering,” *Journal of Composites Science*, vol. 8, no. 12, p. 523, Dec. 2024, doi: 10.3390/jcs8120523.

[14] P. Gouma, R. Xue, C. P. Goldbeck, P. Perrotta, and C. Balázsi, “Nano-hydroxyapatite—Cellulose acetate composites for growing of bone cells,” *Materials Science and Engineering: C*, vol. 32, no. 3, pp. 607–612, Apr. 2012, doi: 10.1016/j.msec.2011.12.019.

[15] V. Bhuvaneshwari, S. Sonia, and D. Sivaganesh, “Harnessing the potency of eco-friendly calcium oxide derived from eggshells for enhanced photocatalytic activity and biocompatibility evaluation in HepG2 cell line,” *Chemical Physics Impact*, vol. 9, p. 100699, Dec. 2024, doi: 10.1016/j.chphi.2024.100699.

[16] M. Heidari, S. Borhan Mousavi, F. Rahmani, and R. Akbari Sene, “Eco-friendly, sustainable and porous eggshell/tea waste-derived CaO nanoparticles as a high-temperature CO2 sorbent: Fabrication and textural/morphological evaluation,” *Journal of Industrial and Engineering Chemistry*, vol. 134, pp. 169–180, Jun. 2024, doi: 10.1016/j.jiec.2023.12.048.

[17] K. H. Min, D. H. Kim, K. H. Kim, J.-H. Seo, and S. P. Pack, “Biomimetic Scaffolds of Calcium-Based Materials for Bone Regeneration,” *Biomimetics*, vol. 9, no. 9, p. 511, Aug. 2024, doi: 10.3390/biomimetics9090511.

[18] R. Donate, R. Paz, Á. Quintana, P. Bordón, and M. Monzón, “Calcium Carbonate Coating of 3D-Printed PLA ScaffoldsIntended for Biomedical Applications,” *Polymers (Basel)*, vol. 15, no. 11, p. 2506, May 2023, doi: 10.3390/polym15112506.

[19] S. M. Sajjadi, M. Haghighi, and F. Rahmani, “On the synergic effect of various anti-coke materials (Ca–K–W) and glow discharge plasma on Ni-based spinel nanocatalyst design for syngas production via hybrid CO2/O2 reforming of methane,” *J Nat Gas Sci Eng*, vol. 108, p. 104810, Dec. 2022, doi: 10.1016/j.jngse.2022.104810.

[20] S. Lu, X. Zhang, and Y. Xue, “Application of calcium peroxide in water and soil treatment: A review,” *J Hazard Mater*, vol. 337, pp. 163–177, Sep. 2017, doi: 10.1016/j.jhazmat.2017.04.064.

[21] S. Pokhrel, “Hydroxyapatite: Preparation, Properties and Its Biomedical Applications,” *Advances in Chemical Engineering and Science*, vol. 08, no. 04, pp. 225–240, 2018, doi: 10.4236/aces.2018.84016.

[22] B. Jiang *et al.*, "An environment-friendly process for limestone calcination with CO2 looping and recovery," *J Clean Prod*, vol. 240, p. 118147, Dec. 2019, doi: 10.1016/j.jclepro.2019.118147.

[23] M. Heidari, S. B. Mousavi, F. Rahmani, T. M. Aminabhavi, and M. Rezakazemi, "Insightful textural/morphological evaluation of cost-effective and highly sustainable Ca-Zr-O nanosorbent modified with the waste date kernel as a biomass pore-former for high-temperature CO2 capture," *Sustainable Materials and Technologies*, vol. 38, p. e00778, Dec. 2023, doi: 10.1016/j.susmat.2023.e00778.

[24] T. Witoon, "Characterization of calcium oxide derived from waste eggshell and its application as CO2 sorbent," *Ceram Int*, vol. 37, no. 8, pp. 3291–3298, Dec. 2011, doi: 10.1016/j.ceramint.2011.05.125.

[25] S.-L. Hsieh *et al.*, "CaO recovered from eggshell waste as a potential adsorbent for greenhouse gas CO2," *J Environ Manage*, vol. 297, p. 113430, Nov. 2021, doi: 10.1016/j.jenvman.2021.113430.

[26] K. Yu, M. L. Dunn, H. Jerry Qi, and K. Maute, "Recent advances in design optimization and additive manufacturing of composites: from enhanced mechanical properties to innovative functionalities," *npj Advanced Manufacturing*, vol. 2, no. 1, p. 26, Jun. 2025, doi: 10.1038/s44334-025-00040-1.

[27] P. H. C. Camargo, K. G. Satyanarayana, and F. Wypych, "Nanocomposites: synthesis, structure, properties and new application opportunities," *Materials Research*, vol. 12, no. 1, pp. 1–39, Mar. 2009, doi: 10.1590/S1516-14392009000100002.

[28] K. Adaikalam, S. Hussain, P. Anbu, A. Rajaram, I. Sivanesan, and H.-S. Kim, "Eco-Friendly Facile Conversion of Waste Eggshells into CaO Nanoparticles for Environmental Applications," *Nanomaterials*, vol. 14, no. 20, p. 1620, Oct. 2024, doi: 10.3390/nano14201620.

[29] W. Alkaron, A. Almansoori, K. Balázsi, and C. Balázsi, "Preparation and Morphology Study of Electrospun Cellulose Acetate Fibers Using Various Solvent Systems and Concentrations," *Periodica Polytechnica Chemical Engineering*, vol. 69, no. 3, pp. 427–438, Sep. 2025, doi: 10.3311/PPch.41199.

[30] W. A. Alkaron, S. F. Hamad, and M. M. Sabri, "Studying the Fabrication and Characterization of Polymer Composites Reinforced with Waste Eggshell Powder," *Advances in Polymer Technology*, vol. 2023, pp. 1–9, Mar. 2023, doi: 10.1155/2023/7640478.

[31] S.-W. Lee, S.-G. Kim, C. Balázsi, W.-S. Chae, and H.-O. Lee, "Comparative study of hydroxyapatite from eggshells and synthetic hydroxyapatite for bone regeneration," *Oral Surg Oral Med Oral Pathol Oral Radiol*, vol. 113, no. 3, pp. 348–355, Mar. 2012, doi: 10.1016/j.tripleo.2011.03.033.

[32] G. N. M. Shan, M. Rafatullah, M. R. Siddiqui, R. T. Kapoor, and M. Qutob, "Calcium oxide from eggshell wastes for the removal of pharmaceutical emerging contaminant: Synthesis and adsorption studies," *Journal of the Indian Chemical Society*, vol. 101, no. 8, Aug. 2024, doi: 10.1016/j.jics.2024.101174.

[33] R. Mohadi, K. Anggraini, F. Riyanti, and A. Lesbani, "Preparation Calcium Oxide From Chicken Eggshells," *Sriwijaya Journal of Environment*, vol. 1, no. 2, pp. 32–35, Aug. 2016, doi: 10.22135/sje.2016.1.2.32-35.

[34] S. Charazińska, E. Burszta-Adamiak, and P. Lochyński, "The efficiency of removing heavy metal ions from industrial electropolishing wastewater using natural materials," *Sci Rep*, vol. 12, no. 1, p. 17766, Oct. 2022, doi: 10.1038/s41598-022-22466-9.

[35] A. Torres-Mansilla *et al.*, "Eggshell Membrane as a Biomaterial for Bone Regeneration," *Polymers (Basel)*, vol. 15, no. 6, p. 1342, Mar. 2023, doi: 10.3390/polym15061342.

[36] A. Jazie, H. Pramanik, A. Sinha, A. A. Jazie, H. Pramanik, and A. S. K. Sinha, "Egg Shell Waste-Catalyzed Transesterification of Mustard Oil: Optimization Using Response Surface Methodology (RSM) optimization of biodiesel production from sewage sludge using RSM View project Development of glycerol based MFC View project Egg Shell Waste-Catalyzed Transesterification of Mustard Oil: Optimization Using Response Surface Methodology (RSM)," 2014, doi: 10.7763/IPCSIT.2012.V56.10.

[37] N. Tangboriboon, R. Kunanuruksapong, and A. Sirivat, "Preparation and properties of calcium oxide from eggshells via calcination," *Materials Science-Poland*, vol. 30, no. 4, pp. 313–322, Dec. 2012, doi: 10.2478/s13536-012-0055-7.

[38] M. H. Kaou, Z. E. Horváth, K. Balázsi, and C. Balázsi, "Eco-friendly preparation and structural characterization of calcium silicates derived from eggshell and silica gel," *Int J Appl Ceram Technol*, vol. 20, no. 2, pp. 689–699, Mar. 2023, doi: 10.1111/ijac.14274.

[39] J. Jitjamnong, "Effect of barium loading on CaO derived from waste egg shell heterogeneous catalyst for canola oil biodiesel," *MATEC Web of Conferences*, vol. 192, p. 03006, Aug. 2018, doi: 10.1051/matecconf/201819203006.

[40] S.-L. Hsieh *et al.*, "CaO recovered from eggshell waste as a potential adsorbent for greenhouse gas CO2," *J Environ Manage*, vol. 297, p. 113430, Nov. 2021, doi: 10.1016/j.jenvman.2021.113430.

[41] K. Adaikalam, S. Hussain, P. Anbu, A. Rajaram, I. Sivanesan, and H.-S. Kim, “Eco-Friendly Facile Conversion of Waste Eggshells into CaO Nanoparticles for Environmental Applications,” *Nanomaterials*, vol. 14, no. 20, p. 1620, Oct. 2024, doi: 10.3390/nano14201620.

[42] U. Nipunika, Y. Jayaneththi, and G. A. Sewwandi, “Synthesis of Calcium Oxide Nanoparticles from Waste Eggshells,” in *2022 Moratuwa Engineering Research Conference (MERCon)*, IEEE, Jul. 2022, pp. 1–5. doi: 10.1109/MERCon55799.2022.9906264.

[43] N. A. Ali, N. Khairuddin, T. S. M. Tengku Azmi, and M. B. M. Siddique, “The Preparation of CaO Catalyst from Eggshells and Its Application in Biodiesel Production from Waste Cooking Oil,” *Arab J Sci Eng*, vol. 48, no. 1, pp. 383–388, Jan. 2023, doi: 10.1007/s13369-022-07125-5.

[44] N. M. Sayed, H. Noby, K. Thu, and A. H. El-Shazly, “High molecular weight cellulose acetate membrane electrospinning: Parameters experimental optimization,” *Mater Today Proc*, Aug. 2023, doi: 10.1016/j.matpr.2023.08.323.

[45] J. M. Deitzel, J. Kleinmeyer, D. Harris, and N. C. Beck Tan, “The effect of processing variables on the morphology of electrospun nanofibers and textiles,” *Polymer (Guildf)*, vol. 42, no. 1, pp. 261–272, Jan. 2001, doi: 10.1016/S0032-3861(00)00250-0.

[46] B. Tarus, N. Fadel, A. Al-Oufy, and M. El-Messiry, “Effect of polymer concentration on the morphology and mechanical characteristics of electrospun cellulose acetate and poly (vinyl chloride) nanofiber mats,” *Alexandria Engineering Journal*, vol. 55, no. 3, pp. 2975–2984, Sep. 2016, doi: 10.1016/j.aej.2016.04.025.

[47] Y. Wang, J. Fu, M. Liu, Q. Fu, and J. Zhang, “Understanding the effect of chain entanglement state on melt crystallization of the polymer freeze-extracted from solution: The role of critical overlap concentration,” *Polymer (Guildf)*, vol. 178, p. 121588, Sep. 2019, doi: 10.1016/j.polymer.2019.121588.

[48] M. S. Azad, “Influence of Polymer Concentration on the Viscous and (Linear and Non-Linear) Viscoelastic Properties of Hydrolyzed Polyacrylamide Systems in Bulk Shear Field and Porous Media,” *Polymers (Basel)*, vol. 16, no. 18, p. 2617, Sep. 2024, doi: 10.3390/polym16182617.

[49] A. Refate *et al.*, “Influence of electrospinning parameters on biopolymers nanofibers, with emphasis on cellulose & chitosan,” *Heliyon*, vol. 9, no. 6, p. e17051, Jun. 2023, doi: 10.1016/j.heliyon.2023.e17051.

[50] S. Tungprapa *et al.*, "Electrospun cellulose acetate fibers: effect of solvent system on morphology and fiber diameter," *Cellulose*, vol. 14, no. 6, pp. 563–575, Oct. 2007, doi: 10.1007/s10570-007-9113-4.

[51] A. Celebioglu and T. Uyar, "Electrospun porous cellulose acetate fibers from volatile solvent mixture," *Mater Lett*, vol. 65, no. 14, pp. 2291–2294, Jul. 2011, doi: 10.1016/j.matlet.2011.04.039.

[52] M. Dhanalakshmi and J. P. Jog, "Preparation and characterization of electrospun fibers of Nylon 11," *Express Polym Lett*, vol. 2, no. 8, pp. 540–545, 2008, doi: 10.3144/expresspolymlett.2008.65.

[53] A. Al-Abduljabbar and I. Farooq, "Electrospun Polymer Nanofibers: Processing, Properties, and Applications," *Polymers (Basel)*, vol. 15, no. 1, p. 65, Dec. 2022, doi: 10.3390/polym15010065.

[54] S. R. K. Vanjari, I. Deepthi, K. Sandeep, B. Amrutur, N. Bhat, and S. Srinivasan, "Bufferless lysis of erythrocytes for isolation of hemoglobin using modified cellulose acetate membranes," *Biotechnology and Bioprocess Engineering*, vol. 17, no. 2, pp. 309–315, Apr. 2012, doi: 10.1007/s12257-011-0452-5.

[55] E. A. Münchow *et al.*, "Synthesis and characterization of CaO-loaded electrospun matrices for bone tissue engineering," *Clin Oral Investig*, vol. 20, no. 8, pp. 1921–1933, Nov. 2016, doi: 10.1007/s00784-015-1671-5.

[56] R. M. Schofield *et al.*, "Driving fiber diameters to the limit: nanoparticle-induced diameter reductions in electrospun photoactive composite nanofibers for organic photovoltaics," *Adv Compos Hybrid Mater*, vol. 6, no. 6, p. 229, Dec. 2023, doi: 10.1007/s42114-023-00788-0.

[57] S. N. Malakhov, S. I. Belousov, A. S. Orekhov, and S. N. Chvalun, "Electrospinning of Nonwoven Fabrics from Polypropylene Melt with Additions of Stearates of Divalent Metals," *Fibre Chemistry*, vol. 50, no. 1, pp. 27–32, May 2018, doi: 10.1007/s10692-018-9922-2.

[58] G. F. Elfawal, A. O. Šišková, and A. E. Andicsová, "Electrospinning: A Game-Changer in Fiber Production and Practical Applications," *Fibers and Polymers*, vol. 26, no. 10, pp. 4133–4160, Oct. 2025, doi: 10.1007/s12221-025-01105-w.

[59] M. M. Ibrahim, T. Y. A. Fahmy, E. I. Salaheldin, F. Mobarak, M. A. Youssef, and M. R. Mabrook, "Role of tosyl cellulose acetate as potential carrier for controlled drug release," *Life Sci J*, vol. 12, no. 10, pp. 127–133, Oct. 2015, doi: 10.7537/marslsj121015.16.

[60] G. Joshi *et al.*, "Transesterification of Jatropha and Karanja oils by using waste egg shell derived calcium based mixed metal oxides," *Energy Convers Manag*, vol. 96, pp. 258–267, May 2015, doi: 10.1016/j.enconman.2015.02.061.

[61] W. Ahmad, S. Sethupathi, Y. Munusamy, and R. Kanthasamy, "Valorization of Raw and Calcined Chicken Eggshell for Sulfur Dioxide and Hydrogen Sulfide Removal at Low Temperature," *Catalysts*, vol. 11, no. 2, p. 295, Feb. 2021, doi: 10.3390/catal11020295.

[62] T. Rasool, S. R. Ahmed, I. Ather, M. Sadia, R. Khan, and A. R. Jafri, "Synthesis and Characterization of Hydroxyapatite Using Egg-Shell," in *Volume 3: Biomedical and Biotechnology Engineering*, American Society of Mechanical Engineers, Nov. 2015. doi: 10.1115/IMECE2015-51933.

[63] D.-N. Phan *et al.*, "Investigation of Mechanical, Chemical, and Antibacterial Properties of Electrospun Cellulose-Based Scaffolds Containing Orange Essential Oil and Silver Nanoparticles," *Polymers (Basel)*, vol. 14, no. 1, p. 85, Dec. 2021, doi: 10.3390/polym14010085.

[64] J. Prakash, K. S. Venkataprasanna, G. Bharath, F. Banat, R. Niranjan, and G. D. Venkatasubbu, "In-vitro evaluation of electrospun cellulose acetate nanofiber containing Graphene oxide/TiO2/Curcumin for wound healing application," *Colloids Surf A Physicochem Eng Asp*, vol. 627, p. 127166, Oct. 2021, doi: 10.1016/j.colsurfa.2021.127166.

[65] C. Silva *et al.*, "Mechanical and Antimicrobial Polyethylene Composites with CaO Nanoparticles," *Polymers (Basel)*, vol. 12, no. 9, p. 2132, Sep. 2020, doi: 10.3390/polym12092132.

[66] S. Tungprapa *et al.*, "Electrospun cellulose acetate fibers: effect of solvent system on morphology and fiber diameter," *Cellulose*, vol. 14, no. 6, pp. 563–575, Oct. 2007, doi: 10.1007/s10570-007-9113-4.

[67] A. Streza *et al.*, "Effect of Filler Types on Cellulose-Acetate-Based Composite Used as Coatings for Biodegradable Magnesium Implants for Trauma," *Materials*, vol. 16, no. 2, p. 554, Jan. 2023, doi: 10.3390/ma16020554.

[68] L. JANOVAK, J. VARGA, L. KEMENY, and I. DEKANY, "Swelling properties of copolymer hydrogels in the presence of montmorillonite and alkylammonium montmorillonite," *Appl Clay Sci*, vol. 43, no. 2, pp. 260–270, Feb. 2009, doi: 10.1016/j.clay.2008.08.002.

Graphical Abstract

Waste eggshells were calcined to obtain CaO particles, which were incorporated into cellulose acetate (CA) solutions (5–20 wt%) using an acetone–acetic acid (2:1) solvent. Electrospinning at 15 wt% CA produced smooth, bead-free fibers with 2–6 % CaO. FTIR confirmed effective CaO integration without altering CA's structure, while XRD revealed reduced crystallinity. The swelling capacity peaked at 710 % for 4 % CaO, demonstrating tunable properties for potential biomedical and environmental applications.

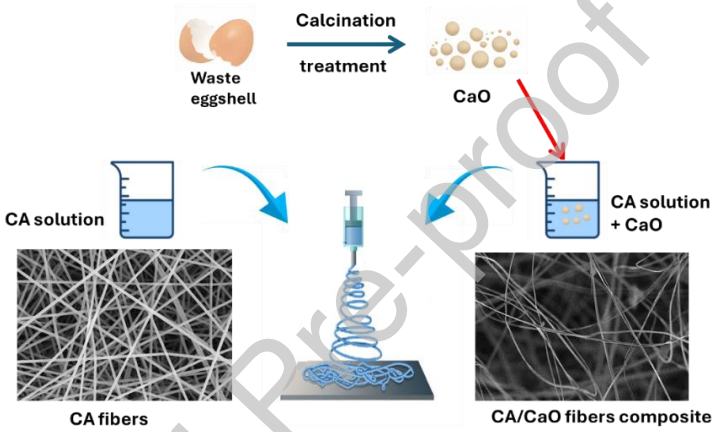

Declaration of Interest Statement

☒ The authors declare that they have no known competing financial interests or personal relationships that could have appeared to influence the work reported in this paper.